

# Synthesis of polyol based Ag/Pd nanocomposites for applications in catalysis



J.A. Adekoya<sup>a,c,1</sup>, E.O. Dare<sup>b</sup>, M.A. Mesubi<sup>a,1</sup>, Adeola A. Nejo<sup>d</sup>, H.C. Swart<sup>e</sup>, N. Revaprasadu<sup>c,\*</sup>

<sup>a</sup> Department of Chemistry, Covenant University, P.M.B. 1023, Ota, Ogun State, Nigeria

<sup>b</sup> Department of Chemistry, Federal University of Agriculture, Abeokuta, Nigeria

<sup>c</sup> Department of Chemistry, University of Zululand, Private Bag X1001, Kwa-Dlangezwa 3886, South Africa

<sup>d</sup> Department of Basic Sciences, Babcock University, Ilishan-Remo, Ogun State, Nigeria

<sup>e</sup> Department of Physics, University of Free State, PO Box 339, Bloemfontein ZA9300, South Africa

## ARTICLE INFO

### Article history:

Received 21 November 2013

Accepted 13 February 2014

Available online 28 February 2014

### Keywords:

Silver

Palladium

Nanoparticles

Polymer stabilised nanoparticles

## ABSTRACT

The synthesis of polyvinylpyrrolidone seed mediated Ag/Pd allied nanobimetallic particles was successfully carried out by the simultaneous reduction of the metal ions in ethylene glycol, diethylene glycol, glycerol, pentaerythritol and sodium borohydride solution. The optical measurement revealed the existence of peak broadening that causes diffusion processes of the metal sols to decrease making it possible to monitor the changes spectrophotometrically. This, together with X-ray diffraction (XRD), X-ray photoelectron spectroscopy (XPS), transmission electron microscopy (TEM) and high resolution TEM measurements strongly support the conclusion that intimately alloyed clusters were formed and the particle growth anisotropy is diffusion limited. Finally, the catalytic potential of the nanocomposites was investigated using 4-nitrophenol in the presence of sodium borohydride at 299 K; a good linear fitting of  $\ln(A/A_0)$  versus the reaction time was obtained, indicating pseudo-first-order kinetics.

© 2014 The Authors. Published by Elsevier B.V. This is an open access article under the CC BY-NC-ND license (<http://creativecommons.org/licenses/by-nc-nd/3.0/>).

## 1. Introduction

Metal nanoparticles composed of two (or more) different metal elements are of interest because of their importance in the improvement of catalysts properties. Bimetallic (or multimetallic) catalysts have long been valuable for in-depth investigations of the relationship between catalytic activity and catalyst particle structure [1,2]. Bimetallic nanoparticles can have the crystal structure which is similar to that of the bulk alloy. In addition, they can adopt another type of structure, in which the distribution of each metal element is not found in the bulk. Such structures, defined by the distribution modes of the two elements, include a random alloy, alloy with an intermetallic compound type, cluster-in cluster, and a core-shell structure of bimetallic nanoparticles [3].

Chia-Cheng et al. [4] synthesised Ag/Pd nanoparticles with a reactive alcohol-type surfactant, sodium dodecyl sulfate (SDS), without the presence of an external reducing agent. Both the UV–Vis absorption spectra and X-ray diffraction (XRD) patterns for the bimetallic and physical mixtures of individual nanoparticles

revealed the formation of a bimetallic structure. Furthermore, the Ag/Pd nanoparticles exhibited distinct catalytic ability for electroless copper deposition [5]. Likewise, dispersed silver/palladium (Ag/Pd) nano platelets were altogether prepared by delivering aliquots of mixed metal nitrates and L-ascorbic acid into a nitric acid solution containing Arabic gum. The shape and size of bimetallic nanoparticles varied with the silver/palladium weight ratio and the concentration of nitric acid. The study concluded that both parameters played a critical role in the nucleation and growth of the Ag/Pd particles [5,6].

Felora et al. also prepared Ag/Pd NPs via a water-in-oil micro-emulsion system of water/dioctyl sulfosuccinate sodium salt (aerosol-OT, AOT)/isooctane at 25 °C, this system was used to produce nanocatalysts for the Heck reactions [7]. Meanwhile, bimetallic Ag/Pd nanoparticles with various concentration ratios of additional silver ions to palladium ions were prepared by a self-regulated reduction method. The size of the bimetallic nanoparticles, was dependent on the molar ratio of  $\text{Ag}^+$  to  $\text{Pd}^{2+}$ . Additionally, the surface plasmon resonance spectra confirmed that the prepared bimetallic nanoparticles were Pd shell-enriched structures [8]. Ag/Pd bimetallic nanoparticles were also prepared from an aqueous solution by the co-reduction of  $\text{AgNO}_3$  and  $(\text{NH}_4)_2\text{PdCl}_6$  in an aqueous solution with TritonX-100. The electrochemical results showed that the Ag–Pd bimetallic nanoalloys possessed a much higher

\* Corresponding author. Tel.: +27 359026152; fax: +27 359026568.

E-mail addresses: [ade.adekoya@covenantuniversity.edu.ng](mailto:ade.adekoya@covenantuniversity.edu.ng) (J.A. Adekoya), [RevaprasaduN@unizulu.ac.za](mailto:RevaprasaduN@unizulu.ac.za) (N. Revaprasadu).

<sup>1</sup> Tel.: +234 17900724.

electrocatalytic activity and better long-term performance than the Ag nanoparticles [9]. Other methods to synthesise Pd/Ag bimetallic nanoparticles include a microwave polyol reduction method [10,11]. The polyols effectively act as bidentate chelating agents for the solvated metal cations and in some cases also serve as reducing and/or stabilising agents once the metal nanoparticles are precipitated.

We have extended the co-precipitation method of Toshima et al. [12–14] to produce novel Ag/Pd nanobimetallic clusters by polymer stabilised and polyol reduction mediated reactions. The reaction conditions were varied by controlling the mixing ratio of the constituent metal salts and reaction temperature. Experimental evidence suggests that the overwhelming majority of precipitation reactions are diffusion-limited. As a result, the concentration gradient and temperature become the predominant factors determining growth rate as a new material is supplied to the particle surface through mass transfer. We have also evaluated the catalytic potential of as prepared  $Ag_{(m)}-M_{(n)}$  bimetallic nanoparticles through the kinetic study of the reduction of p-nitrophenol using UV–Vis spectrometry.

## 2. Experimental

The seed growth or successive addition method was modified from the literature method and used to prepare monodispersed bimetallic Ag/Pd nanoparticles in different polyols at optimum concentration of metal precursors and controlled temperature [15,16]. The reactions for the formation of the bimetallic nanoparticles via anisotropic nucleation and growth are shown in Schemes 1 and 2.

### 2.1. Materials

All inorganic salts, solvents and chemical reagents used were of analytical grade, and were purchased from Sigma–Aldrich Corporation, UK. They are as follow: silver nitrate, palladium (II) chloride, glycerol, ethylene glycol (EG) and diethylene glycol (DEG), pentaerythritol (PET), poly(vinyl pyrrolidone) (PVP), methanol (99.5% w/w) and ethanol (99.5% w/w).

### 2.2. Synthesis of Ag/Pd nanoparticles

The co-precipitation of bimetallic Ag/Pd nanoparticles in the presence of polyvinylpyrrolidone is as follows: 15 mL glycerol (99.5% w/w) was measured in a round bottom flask containing a magnetic stirrer with heating, PVP (0.02–0.06 mmol) was added followed by the injection of PdCl<sub>2</sub> (0.19–0.39 mmol) into the hot solution. The colour rapidly changed to black. The reaction is allowed to proceed for a period of time facilitating the growth of the Pd nanoparticles, which act as the seed. AgNO<sub>3</sub> (0.15–0.57 mmol) was injected into the colloidal mixture and the reaction was continued for 4 h with continuous stirring. After the hot injection of silver nitrate, tint black coloured Ag/Pd sol was obtained and the temperature was maintained till the completion of reaction. While hot, the Ag/Pd sol was copiously washed with methanol several times, and centrifuged at 4400 rpm for 10–

15 min. to remove excess unreacted polymer. The Ag/Pd sol was later redispersed in ethanol.

The above procedure was repeated with ethylene glycol at 160 °C for 3 h and diethylene glycol at 200 °C for 2 h.

The route to prepare bimetallic allied Ag/Pd nanostructured particles in aqueous medium by the seed growth or successive addition method [17] using pentaerythritol (PET) as the capping agent is described as follows: Milliken deionised H<sub>2</sub>O (100 mL) was measured in a round bottom flask containing a magnetic stirrer with heating, PVP (0.02–0.13 mmol) and PET (24.01–37.25 mmol) were added simultaneously. PdCl<sub>2</sub> (0.24–0.36 mmol) was then injected into the hot solution, causing an instant colour change to brown. After the growth of Pd nanoparticles which act as seed, AgNO<sub>3</sub> (0.12–0.82 mmol) was injected into the colloidal mixture, followed by hot injection of NaBH<sub>4</sub> (10 mL, 16.50–18.24 mM) solution. The reaction was continued for 2 h with continuous stirring. The cooled Ag/Pd sol was copiously washed with deionised H<sub>2</sub>O several times, and centrifuged at 4400 rpm for 10–15 min to remove excess unreacted polymer. Then Ag/Pd sol was later re-dispersed in deionised H<sub>2</sub>O.

### 2.3. Isolation of Ag/Pd nanoparticles

The centrifuged sols obtained after decantation is redispersed in double distilled ethanol and cleaned in ultrasonic bath at 50 °C for 60 min before further characterisation of the sols was carried out.

### 2.4. Characterisation

#### 2.4.1. Optical characterisation

A Varian Cary 50 Conc UV–Vis spectrophotometer was used to carry out the optical measurements and the samples were placed in silica cuvettes (1 cm path length), using toluene as a reference solvent. A Perkin–Elmer LS 55 Luminescence spectrometer was used to measure the photoluminescence of the particles. The samples were placed in a quartz cuvette (1 cm path length).

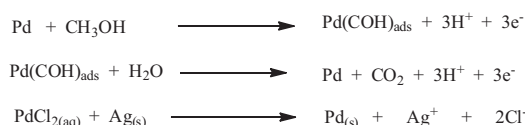
#### 2.4.2. Structural characterisation

The crystalline phase was identified by XRD, employing a scanning rate of 0.05° min<sup>-1</sup> in a 2θ range from 20° to 80°, using a Bruker AXS D8 diffractometer equipped with nickel filtered Cu Kα radiation (λ = 1.5418 Å) at 40 kV, 40 mA and at room temperature. The morphology and particle sizes of the samples were characterised by a JEOL 1010 TEM with an accelerating voltage of 100 kV, Megaview III camera, and Soft Imaging Systems iTEM software. The detail morphological and structural features were investigated using HRTEM images with a JEOL 2010 TEM operated at an accelerating voltage of 200 kV.

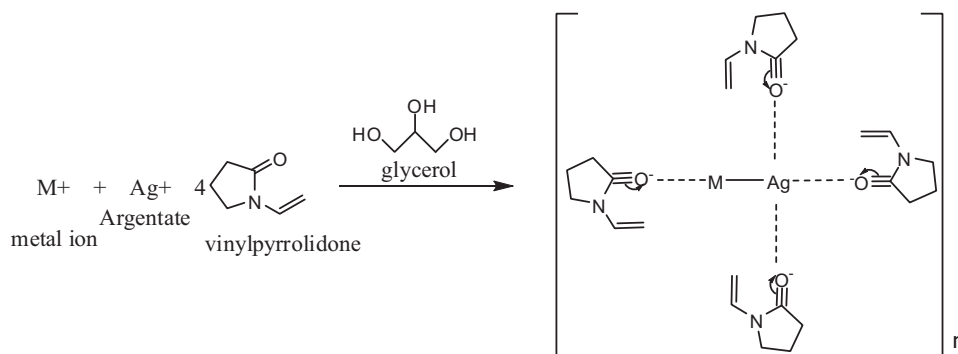
The survey of surface property and high resolution spectra of nanoparticles were collected using XPS PHI 5000 Versaprobe–Scanning ESCA Microprobe, with 100 μm 25 W 15 kV Al monochromatic X-ray beams.

### 2.5. Kinetics of catalytic reduction of p-nitrophenol in the presence of NaBH<sub>4</sub> solution using the prepared Ag/Pd nanoparticles

The catalytic activities of the prepared Ag/Pd nanoparticles stabilised with different matrices (GLY, PET, DEG) were carried out according to Dipak and Misra [18] by measuring NaBH<sub>4</sub> reduction of p-nitrophenol (p-NP) in the presence of Ag/Pd NPs. In order to study catalytic activity, 30 mL of p-nitrophenol (67.05 mM) was mixed with freshly prepared 10.0 ml of aqueous solution of NaBH<sub>4</sub> (0.7 M) with constant stirring in a 250 mL conical flask, while the temperature was maintained at 298–300 K. The prepared Ag/Pd nanoparticles (16.4 mg) were added to the mixture separately and the conical flask was vigorously shaken for mixing. The colour



**Scheme 1.** Redox reactions of Ag seeded AgPd nanoparticle formation.



**Scheme 2.** Reaction for AgM-nanoparticles in PVP stabilising medium with glycerol as reductant.

of the solutions gradually changed from yellow to colourless as the reaction proceeded. The progress of the reaction was monitored by recording the UV–Vis spectra of the solution at a time interval of 120 s. The rate constant of the reduction process was determined by measuring the change in absorbance at 400 nm as a function of time. The controlled experiment was also carried out without AgPd nanoparticles and no change was noticed in the absorption spectra of p-NP. The experiment was repeated using other silver allied nanobimetallic particles in different matrices as previously mentioned.

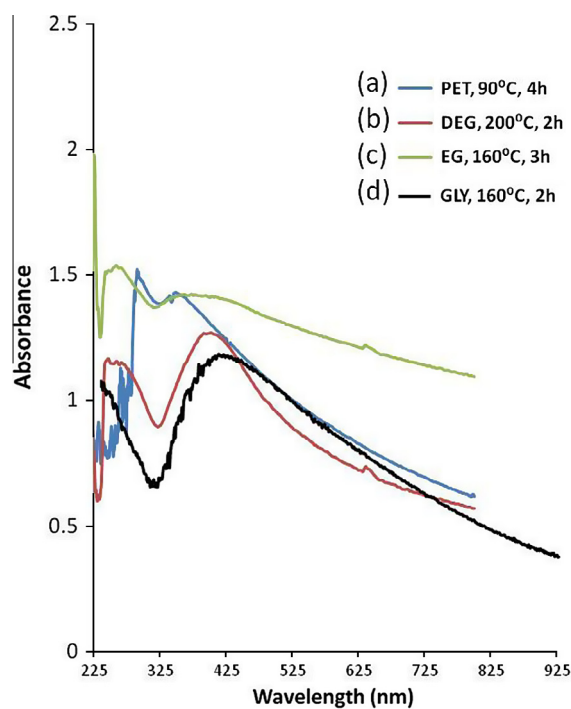
### 3. Results and discussion

The polymer derived polyol stabilised nanoparticles were very stable in both liquid and solid phases. The stability was checked by following the absorbance spectra over extended periods of several months. The oxo groups present in the vinylpyrrolidone stabilised the bimetallic nanoparticles as proposed by Lev and co-workers [19,20]. The use of sodium borohydride resulted in fast reduction of metal ions, but glycerol was the best reducing agent and stabilizer that also acted as a solvent.

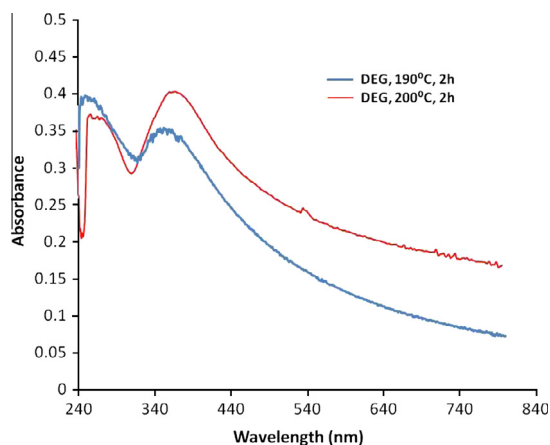
#### 3.1. Optical properties of Ag/Pd sols

Fig. 1 shows the absorption spectra of polyol reduced Pd/Ag in PVP matrix at various temperatures. The surface plasmon absorption for silver usually observed at 400–440 nm is not present but a broad blue shifted absorption peak appears at 335, 378, 336 and 395 nm for pentaerythritol, diethylene glycol, ethylene glycol, and glycerol reductants respectively. The presence of Pd in the bimetallic nanoparticles suppresses the surface plasmon absorption even in the presence of minor quantities [21,22]. The similarity in the shape of the spectra and the absence of any shift of the maximum at all the ratios studied also exclude preferential reduction of Pd ions followed by the reduction of silver which would have resulted in silver-coated Pd clusters. Furthermore, hydrolytic binding of the different polyols onto the substrate (metal-stabilizer) adduct intermediate takes place at different pH and redox potential [23], that also accounts for observed difference in the absorption property and also offers projection to explaining morphological differences in the bimetallic sols. There is no evidence of absorption due to the individual metals which suggests that there is substantial interaction between the particles. There was no effort to reduce the metal ions completely; therefore, there exists a possibility of electron transfer from the metal to unreduced ions.

The effect of change in temperature on the absorption properties of PVP/DEG stabilised Ag/Pd at 200 °C and 190 °C is observed (Fig. 2). There appears no significant difference in their inflection



**Fig. 1.** UV–Vis spectra of AgPd NPs stabilised with (a) PVP/PET, 90 °C, 4 h; (b) PVP/DEG 200 °C, 2 h; (c) PVP/EG, 160 °C, 3 h and (d) PVP/GLY, 160 °C, 2 h.



**Fig. 2.** UV–Vis spectra of AgPd NPs stabilised with PVP/DEG at different temperatures.

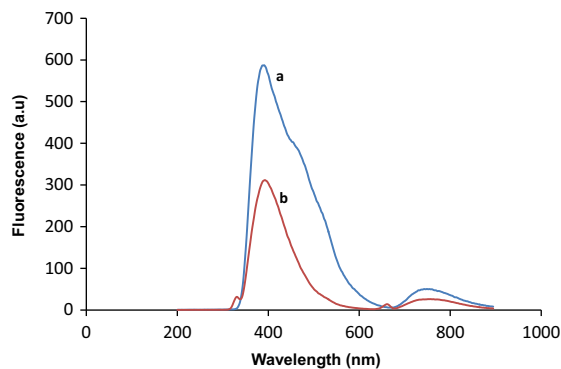


**Fig. 3.** PL spectra of AgPd NPs stabilised with PVP/EG, 1600C, 3 h at excitation wavelengths of (a) 232 nm and (b) 325 nm.

and surface plasmon resonance band which is attributed to the ratio of metal sources, Ag and Pd. In Fig. 3, we observe the congruent nature of the PL emission spectra of Ag/Pd sols prepared in PVP/EG at 160 °C for 3 h: for excitations at 232 and 325 nm, the emission maximum is approximately 382 nm. This agrees with Kasha rule [24] that the emission spectra are usually independent of excitation wavelength, which is an indication of the monodispersity of the nanoparticles [25].

The PL spectra of as prepared polyol reduced composite sols of Ag/Pd stabilised by PVP are shown in Fig. 4. The single  $S_1-S_0$  emission band occurring at 382, 393, 345 and 326 nm for ethylene glycol, pentaerythritol, diethylene glycol and glycerol reductant systems respectively is evidence of the fluorescence property of the nanosols. However, it is observed in Fig. 4 that the stabilizers PVP/GLY and PVP/PET might be responsible for quenching the fluorescence of the nanocomposite resulting in the reduction of the peak intensity in the spectra. We therefore suggest that collisional quenching may possibly result in such observation and formation of excimers at singlet excited states often accounts for this effect [26]. The Pd/Ag sols stabilised by PVP/EG and PVP/GLY have their emission maxima at 385 and 375 nm respectively.

A mirror image relationship in the optical absorbance of Ag/Pd nanosols stabilised with PVP/DEG is observed in Fig. 5. The PL emission maximum is observed at 346 nm, a red shift in relation to the absorption band edge at 383 nm. This is the characteristic Stoke's shift [27,28] showing that the PL emission of the Ag/Pd nanocomposites is actually independent of absorption of light. Further investigation of the optical property led to the estimation of the band gaps of the bimetallic nanoparticles using the direct band gap method [29] which were found to be 3.04 eV (408 nm,  $t = 2$  h), 3.07 eV (404 nm,  $t = 2$  h), 3.00 eV (414 nm,  $t = 3$  h) and 3.47 eV (357 nm,  $t = 4$  h) for PVP/GLY, PVP/DEG, PVP/EG and PVP/PET stabilised AgPd nanoparticles respectively. The absorption edges are red-shifted from that of Ag and Pd bulk crystals given as 3.99 eV and 7.6 eV, respectively [30].

### 3.2. Morphology of the Ag/Pd sols

The representative images in Figs. 6–8 show the TEM and HRTEM micrographs of specific particles of the Pd/Ag nanoclusters stabilised with various capping groups. We observed different shapes peculiar to Pd and Ag metals i.e. spheres (Fig. 6a), cubes (Fig. 7b and Fig. 8d), octahedra (Fig. 8b) and multiply twinned (Fig. 8c) with various degrees of edge and corner truncation. The morphology of the PVP/PET formed bimetallic Ag/Pd clusters as shown in Fig. 6a, has a mean particle size of  $11.64 \pm 2.30$  nm. The particle shape is quasi-spherical and the structural elucidation

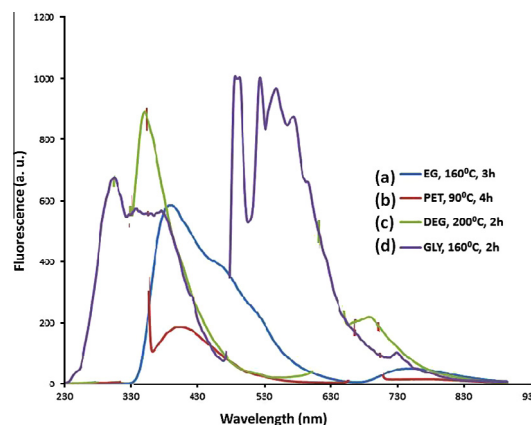


**Fig. 4.** PL spectra of AgPd NPs stabilised with (a) PVP/EG, 160 °C, 3 h; (b) PVP/PET, 90 °C, 4 h; (c) PVP/DEG, 200 °C, 2 h and (d) PVP/GLY 160 °C, 2 h.

based on the HRTEM image (Fig. 6a) reveals the formation of core-shell AgPd nanoclusters.

In Fig. 7, the mean sizes for both large and smaller conjugate particles of PVP/DEG stabilised clusters at 200 °C for 2 h were found to be  $31.47 \pm 7.79$  and  $9.58 \pm 3.09$  nm respectively, forming bimetallic nanoalloys nearly monodispersed with coarse particle size distribution. The average size of PVP/EG stabilised particles at 160 °C for 3 h (Fig. 7c) is  $16.42 \pm 6.13$  nm, with clear evidence of particle agglomeration leading to the formation of alloy nanocages which is kinetically favoured by diffusion limited growth [31]. The HRTEM image (Fig. 8a) shows a contrast in density. This is observed for the Ag/Pd nanoparticles passivated with PVP/GLY (Fig. 8b–d) which confirms the alloy formation whereby the Ag metals appear as dark spots while Pd metals are seen as the brighter conjugates measuring  $15.05 \pm 4.68$  and  $5.37 \pm 1.53$  nm, respectively.

The crystallinity of the as prepared nanoparticles was investigated by powder X-ray diffraction (p-XRD). The PVP/GLY stabilised Ag/Pd NPs at 160 °C for 2 h show characteristic reflections which appear at  $2\theta = 38.51^\circ, 40.33^\circ, 44.49^\circ, 46.55^\circ, 67.68^\circ$  and  $76.92^\circ$  indexed to  $\{111\}$ Ag,  $\{111\}$ Pd,  $\{200\}$ Ag,  $\{002\}$ Pd  $\{220\}$ Pd and  $\{311\}$ Ag crystallographic planes of the fcc structure of Ag/Pd respectively (Fig. 9). Similar planes indexed for both Ag and Pd are observed for PVP/DEG and PVP/EG stabilised Ag/Pd nanoparticles.

This study reveals two factors that are essential in the formation of Ag/Pd alloy cube and polyhedron structures amongst others. The first is the ability of palladium atoms to promote anisotropic growth by inducing structural defects in the silver lattice [32]. The second is the strongly oxidative environment of the

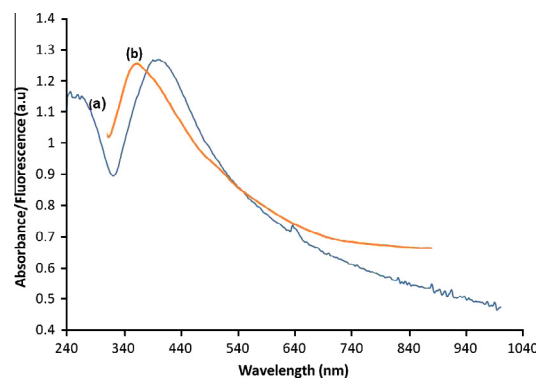


**Fig. 5.** Combined (a) UV-Vis and (b) PL spectra of Ag/Pd PVP/DEG at 200 °C, 2 h.

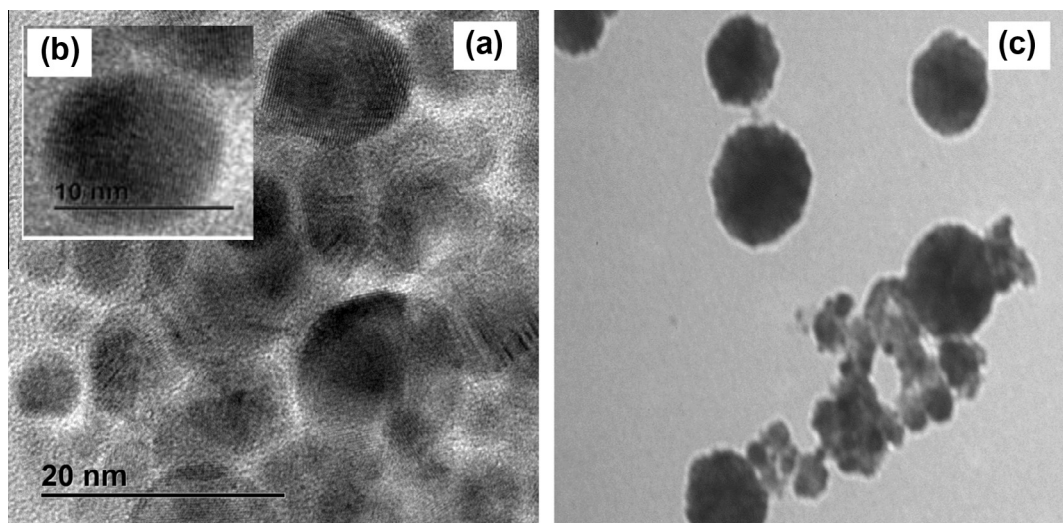


**Fig. 6.** (a) HRTEM image of AgPd NPs capped by PVP/PET at 90 °C, 4 h, (b) inset: showing core-shell nanosphere of AgPd and (c) TEM image of AgPd NPs capped by PVP/PET at 90 °C, 4 h.

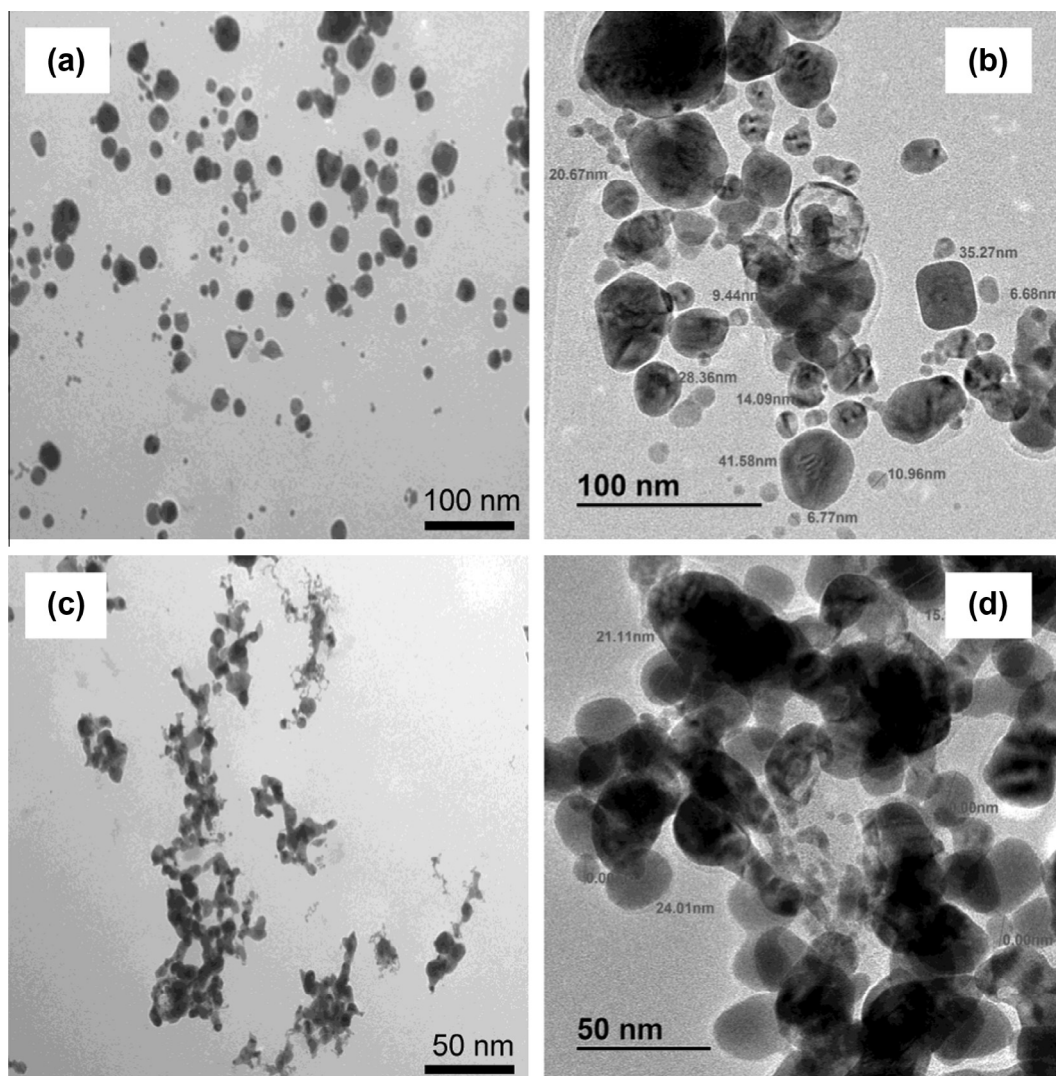


**Fig. 7.** (a) TEM image of AgPd NPs stabilised with PVP/DEG at 2000C, 2 h; (c) TEM image of AgPd NPs stabilised with PVP/EG, 160 °C, 3 h; (b and d) HRTEM images of (a and c), respectively.

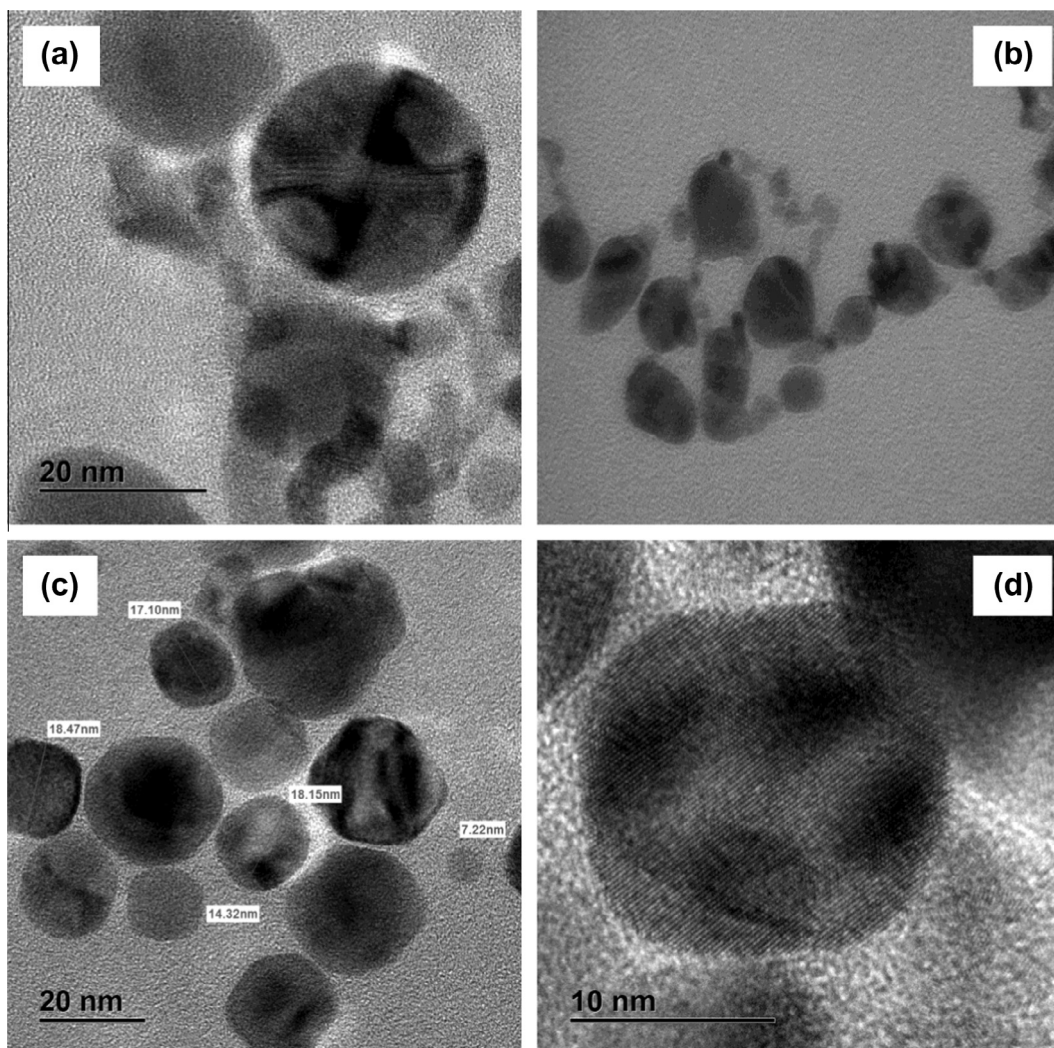


**Fig. 8.** (a) HRTEM image of AgPd NPs in PVP/EG, 160 °C, 3 h, (b) TEM image of AgPd NPs stabilised in PVP/GLY at 160 °C, 2 h, (c) HRTEM image of AgPd in PVP/GLY at 160 °C, 2 h and (d) Close up of particle seen in (c).

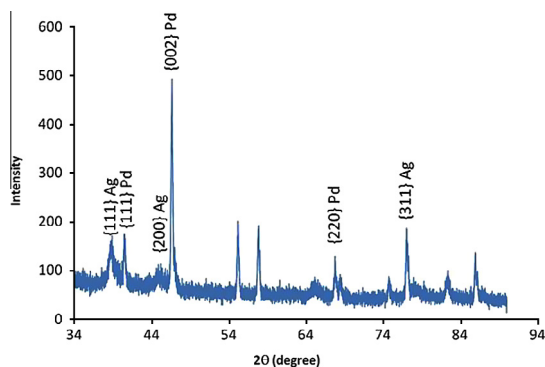


**Fig. 9.** XRD of AgPd nanoparticles stabilised with PVP/GLY at 160 °C, 2 h.

system, which leads to different deposition/dissolution rates for selected crystal facets [33].

A likely source of structural defects is the difference in the reduction kinetics of the two metals. Since the redox potential ( $E^0$ ) of  $\text{Pd}^{2+}/\text{Pd}^0$  system is more electropositive than that of the  $\text{Ag}^+/\text{Ag}^0$  pair (+1.0 V vs.+0.8 V), the nucleation event is dominated by the former. The decrease in the length of the induction period with increased palladium content in the metal nitrate solution confirmed this thermodynamic prediction [34].

### 3.3. XPS results

XPS characterisation for the PVP/DEG stabilised Ag/Pd at 200 °C for 2 h was carried out to study the surface properties of the as-prepared nanoclusters. Fig. 10 shows the high resolution scan and Ag 3d peaks of Ag/Pd nanoparticles. Keeping in mind that the surface was covered by C the surface atomic ratio of Pd to Ag is 0.8:3.9, indicating enrichment of surface of the nanoparticles by Ag.

The integration of the peaks produced a high intensity ratio of  $\text{Ag}^0$  to  $\text{Pd}^0$  which give credence to the formation of nanoalloys very rich in Ag layer, this is in agreement with TEM and HRTEM results in which the polycrystalline nature of the allied AgPd nanocluster revealed a prevalent {111} high index face centred cubic and cuboctahedra structures of Pd alloyed by Ag particles [35–36].

### 3.4. Catalysis study

The rapid catalytic conversion of 4-nitrophenol to 4-aminophenol after addition of Ag allied nanobimetallic particles Ag/Pd was quantitatively monitored as a successive decrease in the peak height at 400 nm (Fig. 11) and the gradual development of new peak at 300 nm which confirmed the formation of 4-aminophenol [37], by a corresponding change in colour of the solution from light

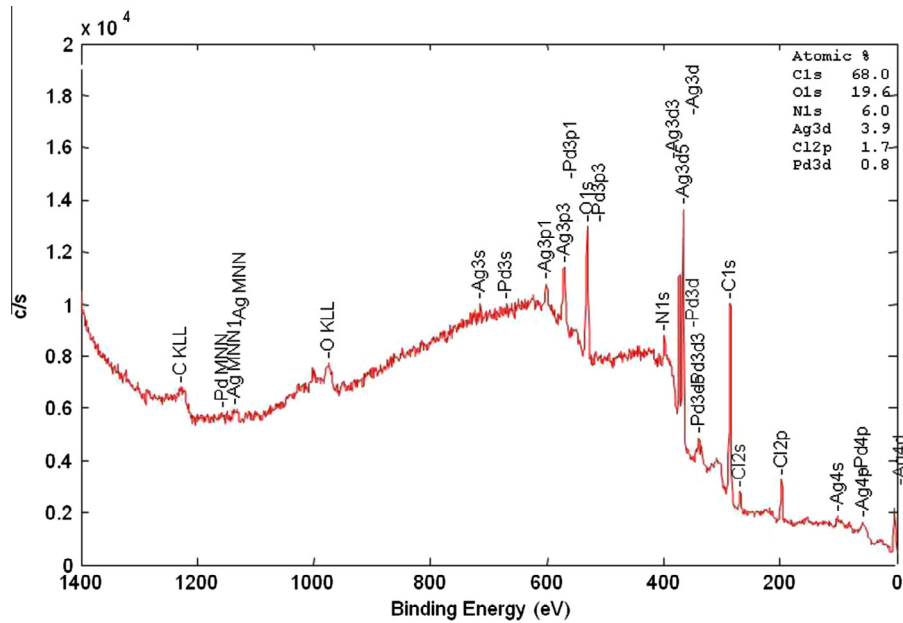


Fig. 10. XPS spectrum of Ag/Pd nanoparticles stabilised with PVP/DEG at 200 °C, 2 h.

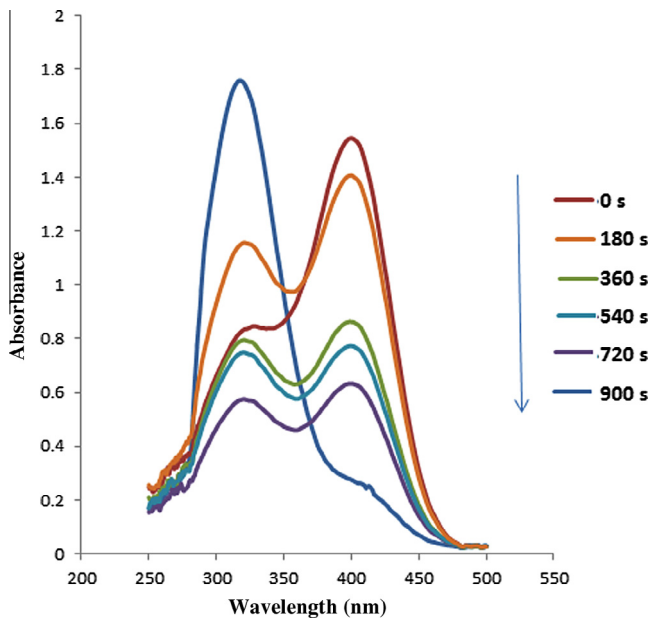


Fig. 11. Change in absorbance at 400 nm as a function of time using AgPd in PVP/GLY at 160 °C, 2 h.

yellow to yellow-green. In this experiment, the concentration of the borohydride ion, used as reductant, largely exceeded that of 4-nitrophenol. As soon as freshly prepared  $\text{NaBH}_4$  solution was added, the Ag/Pd nanoparticles started the catalytic reduction by relaying electrons from the donor  $\text{BH}_4^-$  to the acceptor 4-nitrophenol after the adsorption of both onto the particle surfaces. As the initial concentration of sodium borohydride was very high, it remained essentially constant throughout the reaction.

For the evaluation of catalytic rate, it was reasonable to assume the pseudo-first-order kinetics with respect to 4-nitrophenol. In this regard, since the ratio of absorbance ( $A$ ) of 4-nitrophenol at  $t = t$ , to its value  $A_0$  measured at  $t = 0$  (close to infinity) must be equal to the concentration ratio  $C_t/C_0$  of 4-nitrophenol, the kinetic equation for the reduction is given as:

$$\frac{\partial C_t}{\partial t} = -k_{\text{app}} C_t \text{ or } \ln(C/C_0) = \ln(A/A_0)$$

where  $C_t$  is the concentration of 4-nitrophenol at  $t = t$  and  $k_{\text{app}}$  is the apparent rate constant, which can be obtained from the decrease of the peak intensity at 400 nm with time.

The reaction was completed in minutes at 299 K and did not proceed in the absence of Ag/M/PVP catalyst. A good linear fitting of  $\ln(A/A_0)$  versus the reaction time (s) was also obtained and the pseudo-first-order kinetics was used to calculate the kinetic rate constant. Fig. 12 shows a linear correlation between  $\ln(A/A_0)$  ( $A$ : absorbance at fixed intervals,  $A_0$ : absorbance at time,  $t$  close to infinity) and the reaction time,  $t$  (s) at 299 K. The graph shows that the reaction is a pseudo-first-order [38].

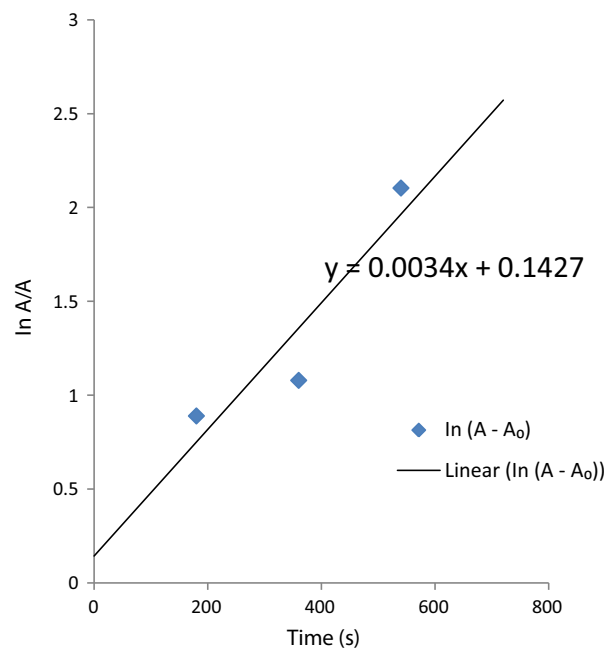


Fig. 12. Plots of  $\ln(A/A_0)$  ( $A$ : absorbance at fixed intervals,  $A_0$ : absorbance at time,  $t$  close to infinity) and the reaction time,  $t$  at 299 K AgPd PVP/GLY, 160 °C, 2 h.

**Table 1**  
Summary of observed rate constant of Ag allied nanobimetallic particles.

Ag allied nanobimetallic particles	Observed rate constant ( $s^{-1}$ )
AgPd/PVP <sub>GLY</sub> , 160 °C, 2 h	$3.4 \times 10^{-3}$
AgPd/PVP/PET <sub>BH</sub> , 90 °C, 4 h	$1.9 \times 10^{-3}$
AgPd/PVP <sub>DEG</sub> , 200 °C, 2 h	$2.9 \times 10^{-3}$

Table 1 shows that there is a significant relationship between nanoparticle quantum size regime and rate kinetic. There is an increase in the kinetic rate constant when bimetallic nanoparticles are used as catalysts instead of their monometallic analogues. Considering the observed rate constants of 4-nitrophenol catalysed reduction at 299 K, Ag/Pd/PVP<sub>GLY</sub> catalyst exhibited a rate constant of  $3.4 \times 10^{-3} s^{-1}$  which was significantly higher than  $2.8 \times 10^{-3} s^{-1}$  reported for Poly(ethylenimine)-Stabilised Ag nanoparticles, but relatively lower than  $9.2 \pm 1.7 \times 10^{-3} s^{-1}$  recorded for AuAg-HNP [39,40].

Furthermore, the rate constant of other Ag allied nanoparticles produced by the polyol reduction route was compared to that prepared in aqueous medium. For instance, the observed rate constant for Ag/Pd/PVP/PET<sub>BH</sub> (90 °C, 4 h) catalyst precipitated from aqueous solution was  $1.9 \times 10^{-3} s^{-1}$ .

The rate constant for the Ag/Pd/PVP<sub>GLY</sub> (160 °C, 2 h) clusters with a particle size of 3.14 nm can be expressed as  $3.4 \times 10^{-3} s^{-1} m^2 L$  per total external surface area of AgPd nanoparticles normalised by unit volume at 299 K. The apparent rate constant per total AgPd,  $k^1$  ( $3.4 - 2.4 \times 10^{-3} s^{-1}$ ), was re-calculated to give  $1.989 \times 10^{-1} s^{-1} m^2 L$  per AgPd surface area. This value was lower compared to  $5.1 \times 10^{-1} s^{-1} m^2 L$  reported by Ballauff and co-workers for the same reaction when polymer mediated Au nanoparticles were used as a catalyst [41].

#### 4. Conclusion

The synthesis of silver palladium nanobimetallic particles by co-reduction and co-precipitation from non-aqueous and aqueous solutions using molecular source precursors and polymer matrix was achieved. Subsequently, characterisation of as prepared nanocomposites was done using optical spectroscopy, electron microscopy, X-ray diffraction (XRD) and X-photoelectron spectroscopy. The derived nanoparticles were investigated for their catalytic potential by reaction of 4-nitrophenol in the presence of sodium borohydride. Stabilisation by PVP was preferred as it was free of agglomeration. The XRD and electron microscopy studies showed evidence for Ag/Pd alloy and core-shell structure formation. This was further corroborated by the XPS measurements. Kinetic studies showed that for alloy formation, the diffusion coefficients need to be many orders of magnitude larger than those of the bulk materials. The bimetallic nanoparticles also showed significant catalytic

activity by the reduction of 4-nitrophenol following pseudo first order kinetics.

#### Acknowledgements

The authors are grateful to the National Research Foundation (NRF), South Africa for funding. The authors also acknowledge the Electron Microscopy Unit, University of Kwa-Zulu Natal and CSIR for the electron microscopy measurements.

#### References

- [1] Sinfelt JH. *J. Catal.* 1973;29:308.
- [2] Sinfelt JH. *Acc. Chem. Res.* 1987;20:134.
- [3] Young-Min C, Hyun-Ku R. *Catal. Surv. Asia* 2004;8:3.
- [4] Chia-Cheng Y, Chi-Chao W, Yung-Yun W. *J. Colloid Interface Sci.* 2004;279:433.
- [5] Chien-Liang L, Yu-Ching H, Li-Chen K. *Electrochem. Commun.* 2006;8:1021.
- [6] Brendan PF, Lu L, G Dan V. *J. Colloid Interface Sci.* 2012;376:62.
- [7] Heshmatpour F, Abazari R, Balalaie S. *Tetrahedron* 2012;68:3001.
- [8] Mizukoshi Y, Fujimoto T, Nagata Y, Oshima R, Maeda Y. *J. Phys. Chem. B* 2012;104:6028.
- [9] Chunling A, Kuang Y, Chaopeng F, Fanyan Z, Wenyang W, Zhou H. *Electrochem. Commun.* 2011;13:1413.
- [10] Kirti P, Sudhir K, Devilal PD, Tulsi M. *J. Chem. Soc.* 2005;117:311.
- [11] Kim SJ, Oh SD, Lee S, Choi SH. *J. Indus. Eng. Chem.* 2008;14:449.
- [12] Toshima N. *Macromol. Symp.* 2008;270:27.
- [13] Toshima N, Kanemaru M, Shiraishi Y, Koga Y. *J. Phys. Chem. B* 2005;109:16326.
- [14] Toshima N, Naoki M, Yonezawa T. *New J. Chem.* 1998;5:1179.
- [15] Toshima N, Kushihashi K, Yonezawa T, Hirai H. *Chem. Lett.* 1989;2:1769.
- [16] Toshima N, Yonezawa T, Kushihashi K. *J. Chem. Soc. Farad. Trans.* 1993;89:2537.
- [17] Viau G, Brayner R, Poul L, Chakroune N, Lacaze E, Fievet-Vincent F, Fievet F. *Chem. Mater.* 2003;15:486.
- [18] Dipak KB, Misra AR. *Carbohydr. Polym.* 2012;89:830.
- [19] Jiang H, Moon K, Wong CP. *Adv. Pack. Mater. Proc. Prop. Interf.* 2005:173.
- [20] Hongjin J, Kyoung-sik-Moon, Li Y, Wong CP. *Chem. Mater.* 2006;18:2969.
- [21] Xu Y, Zhu Y, Zhao F, Ma C. *App. Catal. A General* 2007;324:83.
- [22] Huang YF, Wu DY, Wang A, Ren B, Rondinini S, Tian ZQ, Amatore C. *J. Am. Chem. Soc.* 2010;132:17199.
- [23] Brian L, Vladimir L, Kolesnichenko L, O'Connor J. *Chem. Rev.* 2004;104:3893.
- [24] Lakowicz JR. *Principles of Fluorescence Spectroscopy*. 3rd ed. USA: Springer; 2006. 5.
- [25] Eriksen J, Foote CS. *J. Phys. Chem.* 1978;82:2659.
- [26] Chang SLP, Schuster DI. *J. Phys. Chem.* 1987;91:3644.
- [27] Simonet J. *Electrochem. Commun.* 2009;11:134.
- [28] Zhang G, Kuang Y, Liu J, Cui Y, Chen J, Zhou H. *Electrochem. Commun.* 2010;12:1233.
- [29] Hoffman M, Martin S, Choi W, Bahnmann D. *Chem. Rev.* 1995;95:69.
- [30] Fischer R, Schuppler S, Fischer N, Fauster T, Steinmann W. *Phys. Rev. Lett.* 1993;70:654.
- [31] Wan D, Li Y. *Adv. Mater.* 2011;23:1044.
- [32] Thai-Hoa T, Thanh-Dinh N. *Colloids Surf. B Biointerfaces* 2011;88:1.
- [33] Wook LY, Kim M, Woo Han S. *J. Chem. Soc. Chem. Commun.* 2010;46:1535.
- [34] Brendan PF, Lu L, Dan VG. *J. Colloid Interface Sci.* 2012;376:62.
- [35] Yang CC, Wang Y, Wan C. *J. Electrochem. Soc.* 2005;152:C96–C100.
- [36] Wang Y, Sheng Z, Yang H, Jiang SP, Li CM. *Int. J. Hyd. Energy* 2010;35:10087.
- [37] Rashid M, Bhattacharjee R, Kotal A, Mandal TK. *Langmuir* 2006;22:7141.
- [38] Hashimi ASK, Hutchings GI. *Angew. Chem. Int. Ed.* 2006;45:7896.
- [39] Shin MK, Bommy L, Shi HK, Jae AL, Geoffrey MS, Sanjeev G, Gordon G. *Nat. Commun.* 2012;3:650.
- [40] Kuroda K, Ishida T, Haruta M. *J. Mol. Catal. A Chem.* 2009;298:7.
- [41] Schrinner M, Polzer F, Mei Y, Lu Y, Haupt B, Ballauff M, Gödel A, Drechsler M, Preussner J, Glatzel U. *Macromol. Chem. Phys.* 2007;208:1542.